Charge centers in CaF_2: *Ab initio* calculation of elementary physical properties

M. Letz[1] and L. Parthier[2]
[1]*Schott AG, Research and Development, D-55014 Mainz, Germany*
[2]*Schott Lithotec AG, Otto-Schott Str. 13, D-07745 Jena, Germany*
(Received 5 February 2006; revised manuscript received 2 July 2006; published 31 August 2006)

Charge centers in ionic crystals provide a channel for elementary interaction between electromagnetic radiation and the lattice. We calculate the electronic ground-state energies which are needed to create a charge center—namely an *F* center and an *H* center. In good agreement with common understanding the *F* center results in being accompanied by a small lattice distortion whereas the *H* center is accompanied by a very large lattice deformation. Opposite to the common understanding the additional positive charge in the charge center results rather to be localized on a F_4^{3-} complex than on a F_2^- complex. From the ground states of the charge centers we derive binding energies, diffusion barriers, and agglomeration energies for *M*-center formation. These microscopic quantities are of fundamental interest to understand the dynamic processes which are initiated if the crystals interact with extreme intense deep ultraviolet radiation. We further derive the equilibrium concentrations of charge centers in grown crystals.

DOI: 10.1103/PhysRevB.74.064116 PACS number(s): 78.20.Bh, 71.20.−b, 78.70.−g, 71.15.Mb

I. INTRODUCTION

Calciumfluoride (CaF_2) is a key material for building refractive optical elements in the deep ultraviolet (DUV) range of the electromagnetic spectrum. Especially for structuring microchips an optical system in the DUV range is of extreme technical importance. The reason for this is that the smallest possible structure size, which can be obtained by a microlithographic process, is proportional to the wavelength of the radiation used for structuring. In the last years immense effort has been made in order to provide large single crystals of CaF_2 with high optical quality. These microlithographic processes are performed at wavelengths of excimer laser radiation sources. These are mainly 193 nm (ArF excimer laser), 157 nm (F_2 excimer laser), and 248 nm (KrF excimer laser). CaF_2 is chosen as an optical material due to its cubic crystal structure with (nearly[1,2]) perfect optical isotropy, due to its chemical durability and its mechanical properties which make it applicable for lens fabrication.

Recently high purity single crystals have been grown with impurity concentrations below the ppm level. However, even in these pure single crystals a finite probability for absorption processes remains. Since any absorption process allows for a deposition of energy in the crystal, any energy deposition will in turn lead to a change of material properties. Therefore there exists strong interest to further our understanding of the microscopic mechanism beyond UV absorption in fluoride crystals.

In the past there have been a large number of investigations on charge centers in fluoride crystals in the early 1970s (see, e.g., Refs. 3 and 4). One of the main driving forces at that time was to find materials for color center lasers and hosts which show zero phonon lines for spectral hole burning. Further on CaF_2 is used as a model system for ionic conductivity since the F-sublattice melts approximately 100 K below the melting point of the crystal. Since that time the quality of the crystals has been increased dramatically to the needs of the semiconductor industry for refractive optical materials in the deep UV wavelength range.

Even in an ideal material, where no point defects are present, electromagnetic radiation can be absorbed with a small but finite probability via a two-photon process.[5,6] Such an absorption process will therefore quadratically increase with increasing radiation intensity and becomes of strong importance with increasing radiation intensity. Such a two-photon process will separate charges and will create an electron-hole pair, provided the sum of the energy of the two photons exceeds the 11.2 eV of the excitonic two-particle bound state of the Γ exciton.[7] Above this energy a large probability for absorption is present.[8] The charges of the electron and the hole have further the possibility to lower their energy by distorting the surrounding lattice. This means that a localization of the electron-hole pair takes place together with a lattice distortion. The resulting state is called an *F-H* pair[9,10] or a self-trapped exciton (STE).[11] This *F-H* pair can recombine with an optically forbidden transition, which leads to the fluorescence at 278 nm with a relatively large lifetime at room temperature of 1.1 μs.[9,12–14]

In a real material there are a number of defects present. In this case the defect concentration is governed by entropy. The concentration at room temperature is in this case not necessarily determined by its room-temperature equilibrium value. This is due to the fact that the system falls with respect to defect statistics out of equilibrium already at the crystallization point where defect diffusion becomes strongly hindered.

At high radiation rates the creation of *F-H* pairs provides the major source towards radiation dependent change of optical material properties of CaF_2. Due to thermal diffusion the charge centers can move around in the material. Above 170 K,[15] the charge centers are known to be mobile. This mobility increases on one site the probability of recombination of *F* and *H* centers. On the other site mobile charge centers can be trapped by point defects and impurities in the material which can lead to room-temperature stable charge centers. This temperature dependence is a strong hint that activation energies for diffusive transport of charge centers are of crucial importance when understanding radiation dependent change in material properties of CaF_2. In the present

paper we calculate energies for charge center formation and derive the necessary microscopic parameters for charge center diffusion.

The paper is organized as follows: In Sec. II we phenomenologically describe the interaction between radiation and the fluoride crystal. In Sec. IV we discuss the band structure of CaF_2 which is needed as a starting point when investigating the localized charge centers. In the next Sec. V we report calculation on a larger unit cell up to $Ca_{108}F_{216}$ where either one fluor ion is removed and an electron is localized on the vacancy or where an additional fluor ion has been added forming an essentially positively charged complex where the hole is localized. The lattice deformation is discussed in Sec. V D and the obtained electronic structure in Secs. V A and V C. In Sec. V E we calculate the equilibrium concentrations of F and H centers in an as-grown crystal.

II. INTERACTION OF UV RADIATION WITH CaF_2

For a qualitative understanding of the dynamic processes involving charge center formation and charge center motion we follow the arguments of Ref. 16. We assume that a two-photon process creates a pair of an F center and a H center which are spatially uncorrelated. There is further no long-range interaction between these pairs, an assumption which is physically justified by the screening of the Coulomb potential.

Further, all interaction between the F and H centers is neglected. That means we assume a uniform density for both centers. This approximation gets exact in the dilute limit. This means that the two-particle correlation functions $g_{\kappa,\kappa'}(r)$ is assumed to have the uniform value 1. As the only driving force for F-H-pair recombination we assume statistical fluctuations of the charge center positions,

$$\rho^{(2)}_{\kappa,\kappa}(r) = \rho^{(1)}_{\kappa} g_{\kappa,\kappa}(r) \approx \rho^{(1)}_{\kappa} \quad \kappa \in \{F,H\} \tag{1}$$

and for the nondiagonal correlation function we assume

$$\rho^{(2)}_{F,H}(r) = \rho^{(2)}_{H,F}(r) \approx \sqrt{\rho^{(1)}_{F} \rho^{(1)}_{H}}. \tag{2}$$

With the above approximations we can directly write down a system of rate equations for the creation of F and H center in the ideal material,

$$\frac{\partial \rho^{(1)}_{\kappa}}{\partial t} = I^2 p - K \sqrt{\rho^{(1)}_{F} \rho^{(1)}_{H}} \quad \kappa \in \{F,H\}. \tag{3}$$

The first term on the right side creates pairs of F and H charge centers. This creation goes via a two-photon process and is therefore proportional to the squared radiation intensity I^2. The second term on the right side of Eq. (3) describes the recombination of particles. This recombination is proportional to the probability of finding two particles within a distance smaller than the recombination radius r_0 and is proportional to the effective recombination rate K,

$$K = 4\pi r_0 (D_F + D_H). \tag{4}$$

Here D_F and D_H are the diffusion constants for F-center and H-center diffusion. The temperature dependence of these diffusion constants is known from Ref. 17 as

$$D_{\kappa} = d_{\kappa} e^{-E_{\kappa}/k_B T} \tag{5}$$

with E_F=0.7 eV and E_H=0.46 eV. In order to obtain microscopic information on the material parameters needed for charge center diffusion, we do an *ab initio* calculation of the charge centers together with the resulting lattice distortions. Among other results we also confirm a well-known result[3] that there is a strong asymmetry between the number of F centers and H centers in CaF_2. At the melting point of the F sublattice, where the system falls out of equilibrium with respect to its defect concentration, there is already a reasonable number of F centers present but there are practically no H centers (see Sec. V E).

III. METHOD OF CALCULATION

In the present work we use a commercially available density-functional package (VASP).[18] The code is a plane-wave code which uses ultrasoft pseudopotentials. The generalized gradient approximation (GGA) is used to calculate the exchange correlation energy. Through most of the calculation we set the plane-wave cutoff for the numerical evaluation of the electron density to 500 eV. This was due to restriction of computer time. In Appendix A we show that this choice is in general sufficient. For the larger clusters with 32 Ca ions and 64 F ions in Sec. V we perform a Γ-point calculation, which corresponds to a k mesh of 0.575 $Å^{-1}$. The criterion for the electronic convergence was set to $\Delta E/E = 10^{-6}$.

IV. BAND STRUCTURE OF CaF_2

As a starting point the band structure of CaF_2 has been calculated. The resulting band structure is in good agreement with experiments and other *ab initio* calculations.[19] As expected for a pure DFT (density functional theory) calculation the resulting band gap is with 7.7 eV too small compared with the 11.8 eV which are measured experimentally (see Fig. 1).

A screened exchange calculation improves the too small band gap.[19] Also a similar calculation which uses an interpolation between DFT and Hartree-Fock approximation[24] arrives at a similar result. Details on the band structure together with a calculation of phonon modes which are compared to neutron-scattering results can be found in Ref. 20. In Ref. 21 also mechanical properties of CaF_2 and other fluorites are calculated.

V. STRUCTURE OF F AND H CENTER

In order to calculate charge centers we set up a cluster of $Ca_{32}F_{64}$ using periodic boundary conditions. Due to the large size of the elementary cell calculations are performed using one k point only (Γ-point calculation). Removing one F atom and allowing for a relaxation of the structure into the energy minimum gives an F center. Adding an F atom and allowing for structural relaxation is a configuration of an H center. For the structural relaxation, which takes account of the lattice deformation, the size of the elementary cell was kept fixed. In order to obtain charge neutrality in the clusters an extra positive charge is trapped near the additional F ion and an

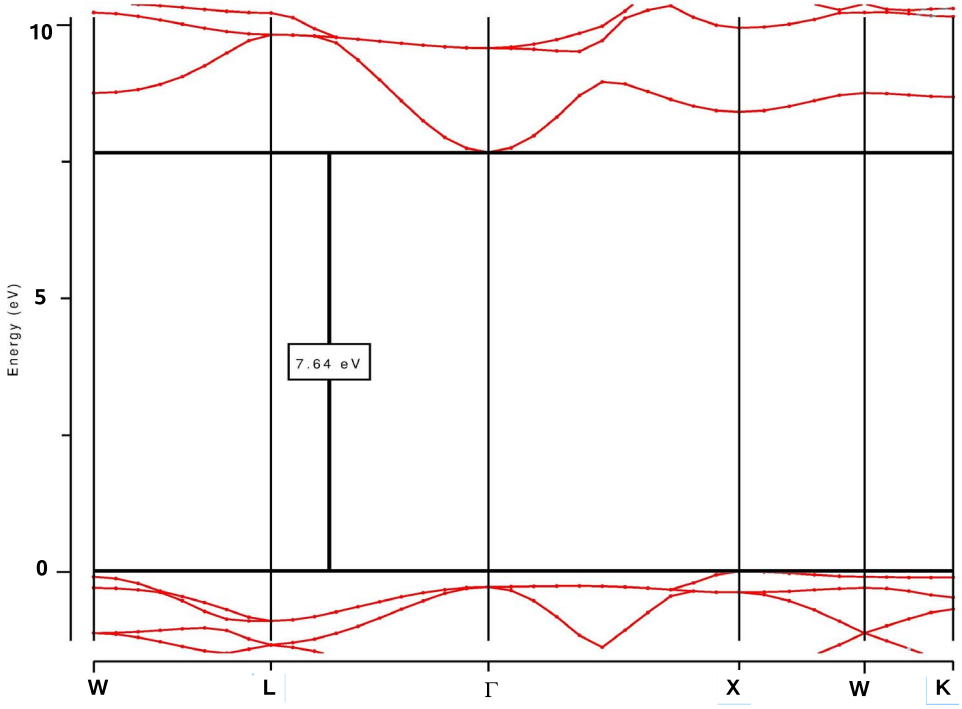

FIG. 1. (Color online) Band structure of CaF_2 from an LDA calculation. As expected the band gap results in a too small value, whereas the main features, e.g., like the indirect transitions, are obtained in good agreement with experiments.

extra negative charge is trapped in the F-ion vacancy. Due to the periodic boundary conditions a periodic array of charge centers is calculated where the distance is equal to four lattice constants. Since the electronic wave functions of such local defects drop off exponentially there should be a small but finite interaction between the charge centers. A check for finite-size effects due to defect-defect interaction is made using larger systems of $Ca_{108}F_{216}$ cluster and shown in Sec. V F.

A. F^- center

Removing one F atom leads to a cluster with $Ca_{32}F_{63}$. Since the F atom had an electron closely attached to it, this electron is now localized in the F vacancy. A defect level with an exponentially decaying wave function is created in the band gap, where the chemical potential moves in. This leads to a half filled single electron level, where the electron can be excited with a photon leading to an absorption in the optical transmission spectrum. Such a half filled state has a spin of $S=1/2$ which makes it possible for spin-resonance measurements[22] to observe the defect. As a next step a relaxation of the structure is performed. As a result there is only minor change in the structure. The electronic band structure of the resulting defect is plotted in Fig. 2. The resulting change in electronic density compared to the undisturbed configuration is shown in Fig. 3. The additional charge is well localized at the defect and only weak lattice distortion is seen. The symmetry of the F center is tetrahedron symmetry T_d. In Appendix B we calculate the splitting of excited energy levels due to the tetrahedron symmetry using arguments from group theory.

B. M center

A pair of two F centers is called an M center. Usually entropy will be the dominant driving force for a homogeneous distribution of F centers. On the other hand the overall lattice distortion which is needed to trap an electron as an F center can be reduced if two F centers join forming an M center. By removing a second F^- ion from our cluster with periodic boundary conditions we create an M center, whereby the two F centers can be oriented along different directions in the crystal. We investigate M centers in the 100, the 110, and 111 directions. In the latter case we have two possibilities: one where a Ca^{2+} is in between the two missing F^- ions and the second one with an empty space in between. By calculating the difference in total energy between an M center ($Ca_{32}F_{62}$) and a $Ca_{32}F_{64}$ cluster in comparison with twice the total energy of an F-center configuration we obtain an expression for the agglomeration energy of two F centers forming an M center,

$$\Delta E_{M-aggl} = E_{Ca_{32}F_{62}} + E_{Ca_{32}F_{64}} - 2E_{Ca_{32}F_{63}}. \quad (6)$$

We can think of this configuration as taking two F centers infinite distance away from each other and comparing this state with two F centers on nearest- (or next-nearest- or next-next-nearest-) neighbor sites. The result is summarized in Table I. The configuration where the two F centers are on nearest-neighbor sites oriented along the 100 direction is the most preferred one.

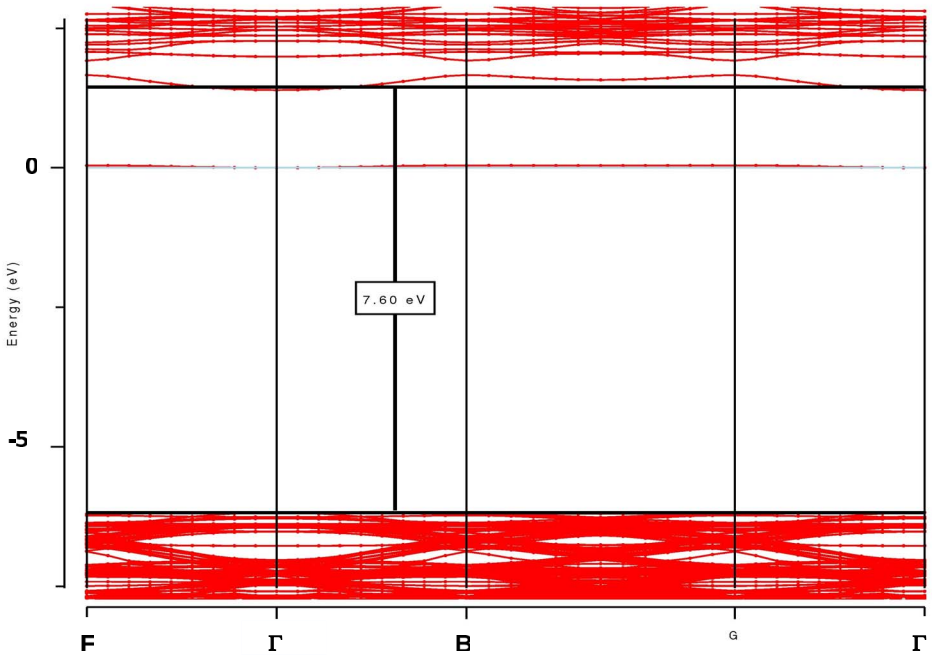

FIG. 2. (Color online) Band structure of $Ca_{32}F_{63}$ from an LDA calculation. A weakly dispersive defect level shows up in the band gap. the Fermi level marked as 0 of the energy scale is in the half filled defect level indicating a free spin of the defect.

C. *H* center

For a configuration which is used as a starting point for the H^+ center, an F ion is replaced by a pair of F ions where according to Ref. 12 the line connecting the two F atoms points along the 110 direction. In this way a $Ca_{32}F_{65}$ cluster is obtained. After a relaxation of the structure a stable configuration with localized defect level in the band gap is obtained. The resulting band structure is plotted in Fig. 4. The charge distribution is plotted in Fig. 5. The additional positive charge is located in the center of four F^- ions. In this way an F_4^{3-} complex is created. This is opposite to the standard literature,[3,23] e.g., where the *H* center is described as a F_2^- complex. The result of the calculation is very clear therefore there is little doubt on the quality of the result. In the 1970s when the microscopic models of the charge centers in fluoride crystals were developed, there was no possibility to perform such a detailed microscopic calculation. The details of the geometry of the four F ions which form the F_4^{3-} center is plotted in Fig. 6. One can further see that the *H* center is accompanied by a very large lattice distortion. This means that a large part of the energy, which is needed to create a localized but unbound electron-hole pair originates from lattice distortion around the *H* center. Therefore the main part of the energy which is gained by trapping an electron-hole pair as a self-trapped exciton (STE) comes from the release of the lattice distortion around the *H* center when an *F* center is close. In addition this is the reason why it was not possible in the past to observe single *H* centers. Usually a crystal is cooled down from the melting point and falls out of thermodynamic equilibrium with respect to its defect concentration at a temperature which is shortly below the melting point. At that temperature a large number of F^- vacancies is present but only a very small number of interstitial F ions. This means that the crystal even at the slowest cooling rates never reaches its thermodynamical equilibrium at zero temperature, where each F^- position is occupied by an F ion. In fact there

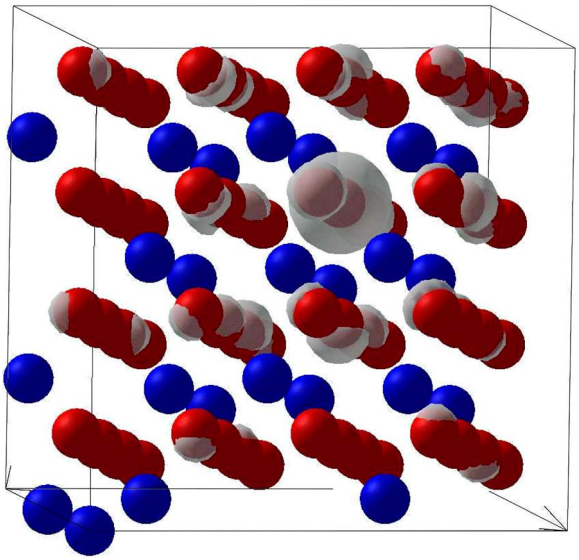

FIG. 3. (Color online) Change in electronic density due to formation of an *F* center. The *F* center is well localized and accompanied by only a very small lattice distortion.

TABLE I. Agglomeration energy for the formation of an *M* center in CaF_2. According to our result in the most favored configuration the two F vacancies are oriented along the 100 direction. In this direction the gain due to lattice relaxation is largest.

Type of *M* center	$\Delta E_{M\text{-}aggl}$ /eV
M 100	−0.85
M 110	−0.14
M 111 (Ca)	−0.31

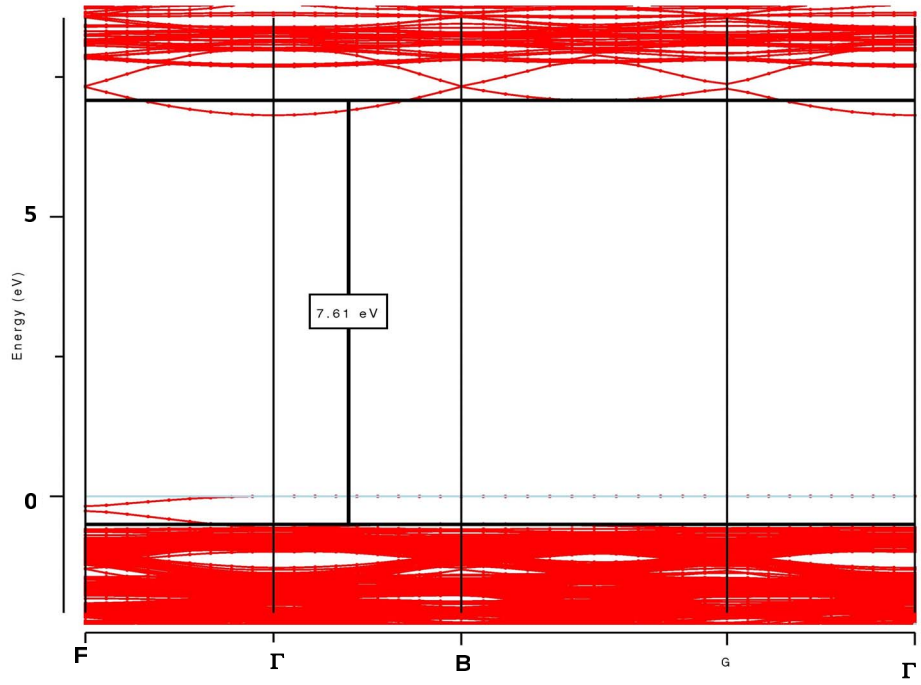

FIG. 4. (Color online) Band structure of $Ca_{32}F_{63}$ from an LDA calculation. A weakly dispersive defect level shows up in the band gap. The Fermi level marked as 0 of the energy scale is in the half filled defect level indicating a free spin of the defect.

will be a reasonably large number of F^- vacancies. By heating the crystal and quenching it down to liquid-nitrogen temperatures it is possible to additively color the system by creating *F* centers. This argument is quantified in more detail in Sec. V E. A defect which is discussed in CaF_2 as well is the v_k center. In the v_k center two F^- ions are shifted out of their equilibrium positions forming an F_2^- molecule. We did not find a stable configuration for such a bare center and believe that it is only stabilized in the vicinity of dopant ions.

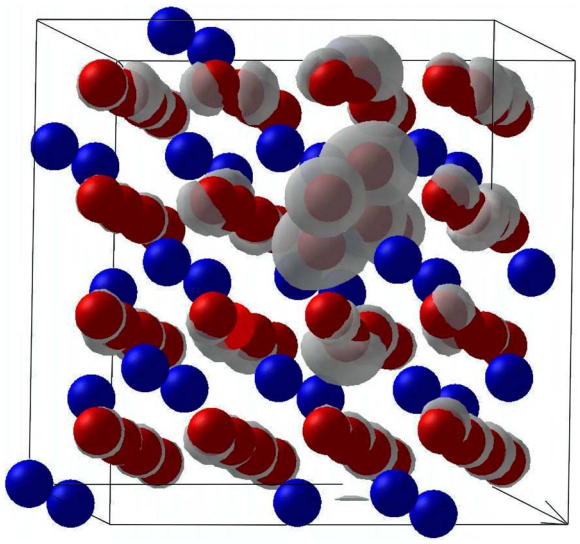

FIG. 5. (Color online) Change in electronic density due to formation of an *H* center. The *H* center is well localized and accompanied by a huge lattice deformation. The additional positive charge is located at the center of four F^- ions forming a F_4^{3-} complex. The symmetry of the *H* center is C_{2v}. In Appendix B we estimate the level splitting due to symmetry arguments.

D. Lattice relaxation

In the following the energy to create an electron-hole pair in the form of an *F-H* pair is calculated. This is the total energy of an *F-H* pair. The undisturbed lattice has a total energy of −17.64 eV per CaF_2 unit. For a $Ca_{32}F_{64}$ this is $-17.64\times 32=-564.63$ eV. An *F-H* pair which has infinite distance is the electronic and fully converged structure of a $Ca_{32}F_{63}$ cluster plus the structure of a $Ca_{32}F_{65}$ cluster,

$$\begin{aligned}\Delta E_{F\text{-}H} &= 2E_{Ca_{32}F_{64}} - E_{Ca_{32}F_{63}} - E_{Ca_{32}F_{65}} \\ &= 2564.63 - (-556.01) - (-565.08)\ \text{eV} \\ &= -8.17\ \text{eV}, \end{aligned} \tag{7}$$

via an optically forbidden transition the *F-H* pair can recombine with the relative long lifetime of 1.1 μs and finally relax into the undisturbed configuration. The STE fluorescence which corresponds to the *F-H*-pair recombination is known to be at 278 nm.[13] In Fig. 7 we show a schematic plot of the energy scheme which relates the measured 278 nm which is a photon energy of 4.463 eV to the calculated energy difference of 8.17 eV.

E. Equilibrium concentrations of charge centers in a grown crystal

In Secs. V A and V C we saw that there is a strong asymmetry in the energy which is needed to produce an *F* or *H* center. The main reason for this asymmetry lies in the strong lattice distortion which results when adding an F ion into an interstitial lattice site in order to create an *H* center. We now estimate the concentration of the *F* and *H* centers which is obtained when the system falls out of equilibrium. Therefore we compare the total energy of fluorine in the four possible

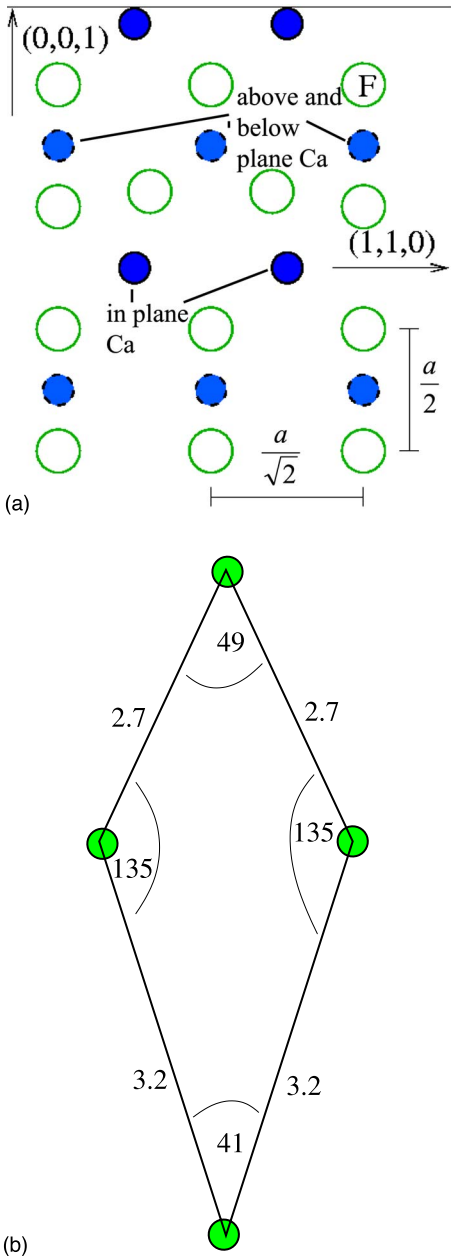

FIG. 6. (Color online) The geometry of the F_4^{3-} H center as it lies in the $(-1,1,0)$ plane is shown. The angular as they result from the calculation are plotted and given in ° in (a). The distances between the four F ions are given in Å. The four F ions form a perfect plane above and below which a Ca^{2+} ion is located. The overall symmetry of the H center obtained via our calculation is C_{2v} as can be seen from (b).

configurations: (i) as fluor in the regular CaF_2 lattice, (ii) as fluor in an interstitial lattice site, (iii) the energy gain which is obtained when removing a F^- ion in order to create an F center, and (iv) the fluor in the F_2 atom of gaseous fluor. From Sec. V D we know that the energy which is needed to create an F-H pair is 8.17 eV. We now ask how this energy is distributed between the F and the H centers. For the F center we obtain

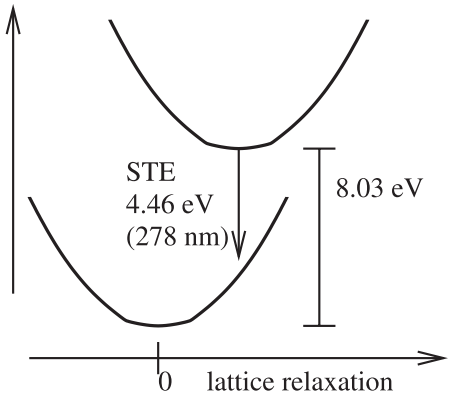

FIG. 7. Schematic plot of the energy levels of the F-H pair before and after recombination. Resulting from the calculation there is a large part of the energy stored in a lattice deformation (Stokes shift). Therefore the measured 278-nm fluorescence is smaller than the calculated energy difference of 8.17 eV.

$$\Delta E_F = \left(E_{Ca_{32}F_{64}} - \frac{1}{2}E_{F_2} - E_{Ca_{32}F_{63}}\right) - \Delta E_{F\text{-}H}$$
$$= [-564.63 - (-1.79) - (-556.01)] - (-8.17)\ \text{eV}$$
$$= 1.35\ \text{eV}, \quad (8)$$

which is the energy gain when creating the F center and forming half of a F_2 molecule. In Ref. 24 a much larger value ($\approx$7.9 eV) is obtained for F^--center formation by comparing to the energy of a bare F atom instead of a F_2 molecule. This is in agreement with older *ab initio* studies,[25] where small clusters of only 18 ions were studied and a diffusion activation energy for the F center of 1.69 eV results. For the H center we obtain in a similar way

$$\Delta E_H = \left(E_{Ca_{32}F_{64}} + \frac{1}{2}E_{F_2} - E_{Ca_{32}F_{65}}\right) - \Delta E_{F\text{-}H}$$
$$= [-564.63 + (-1.79) - (-565.08)] - (-8.17)\ \text{eV}$$
$$= 6.82\ \text{eV}. \quad (9)$$

The sum of both energies gives 8.17 eV which is the energy needed to create an F-H pair. In principle one should add in Eq. (8) and subtract in Eq. (9) the chemical potential of a corresponding F_2 gas phase, which in general depends on temperature and pressure, $\Delta E_F \rightarrow \Delta E_F + \mu(T,p,N)$ and $\Delta E_H \rightarrow \Delta E_H - \mu(T,p,N)$. For simplicity and due to a lack of knowledge of the detailed environment, we set this term to zero. The point where the system falls out of equilibrium with respect to its F-ion concentration is given by the melting temperature of the fluor sublattice in CaF_2. This occurs at approximately 1500 K which is 150 K below the melting point of the crystal. At this temperature the equilibrium concentration of F center is

$$\langle n_{eq}^F \rangle = \frac{1}{v_0} e^{-\Delta E_F/k_B T} = 2.5 \times 10^{23}\ \text{m}^{-3} = 2.5 \times 10^{17}\ \text{cm}^{-3}, \quad (10)$$

and for the H center also at a temperature of 1500 K it is

TABLE II. For *F* and *H* centers the equilibrium concentrations at different temperatures are calculated. The results are given as well in absolute concentrations (cm^{-3}) as well as in molar fractions (ppm).

		$n_{eq}(T=300\ \mathrm{K})$		$n_{eq}(T=1500\ \mathrm{K})$		$n_{eq}(T=1650\ \mathrm{K})$	
Dopant	ΔE_{defect}/eV	/m^{-3}	/ppm	/m^{-3}	/ppm	/m^{-3}	/ppm
F center	−1.35	2.49×10^{4}	9.74×10^{-19}	1.29×10^{23}	5.04	3.43×10^{23}	13.4
H center	−6.82	1.75×10^{-91}	6.84×10^{-114}	1.20×10^{4}	4.70×10^{-19}	1.72×10^{6}	6.72×10^{-17}

$$\langle n_{eq}^{H}\rangle = \frac{1}{v_0}e^{-\Delta E_H/k_BT} = 1.2\times10^{4}\ \mathrm{m}^{-3} = 0.012\ \mathrm{cm}^{-3}, \tag{11}$$

where $v_0=a^3=(5.46\times10^{-10})^3\ \mathrm{m}^3=1.67\times10^{-28}\ \mathrm{m}^3$ is the volume of the elementary cell. This result means that in ideally grown crystal there is already a strong asymmetry between fluor vacancies and fluor interstitial. There are practically no *H* centers but already a finite number of *F* centers. Using the molar weight, the density of CaF_2, and the Avogadro constant, NA, we can calculate the molar concentration of charge centers in thermal equilibrium at different temperatures and as well an absolute particle number in ppm. This is done in Table II. To calculate the equilibrium densities in ppm we used

$$\langle n_{eq.}^{H/F}\rangle^{\mathrm{ppm}} = \langle n_{eq.}^{H/F}\rangle\frac{u_{CaF_2}}{\rho \mathrm{NA}}, \tag{12}$$

where $u_{CaF_2}=78.08\ \mathrm{g/mol}$ is the molar weight of CaF_2, $\rho=3.31\ \mathrm{g/cm}^3$ is the density of CaF_2, and NA is the Avogadro number.

There is even a very small but finite change in the density of the material due to the equilibrium concentration of F vacancies. This change in density is

$$\Delta\rho = 19.00\ \mathrm{g/mol}\frac{\langle n_{eq}^{F}\rangle}{\mathrm{NA}} = 19.00\frac{2.5\times10^{17}}{6.022\times10^{23}}\ \mathrm{g/cm}^3$$
$$= 7.9\times10^{-6}\ \mathrm{g/cm}^3 = 7.9\times10^{-3}\ \mathrm{kg/m}^3. \tag{13}$$

From that follows that an extremely inhomogeneous distribution of charge centers can in principle have an influence on the density homogeneity of the material and therefore also on the refractive index homogeneity. Since, however, the bare charge centers are mobile at room temperature, this process will lead to a homogeneous distribution already.

F. Finite-size effects

In order to estimate finite-size effects we configured a larger cluster with $Ca_{108}F_{216}$ for the unperturbed configuration. In this cluster the resulting configuration for the *F* center and for the *H* center from the smaller clusters was inserted. For these calculations we restricted ourselves to a plane-wave cutoff of 400 eV only due to limitations of computer power. After this first one electronic configuration was performed and the forces on the ions were calculated. As a result there is still a non-negligible finite-size effect present. For the *F* center we obtain

$$\Delta E_{fin\text{-}size}^{F\ elec\text{-}relax} = 76E_{CaF_2} + E_{Ca_{32}F_{63}} - E_{Ca_{108}F_{215}}^{elec\text{-}relax}$$
$$= -1902.59 - (-1908.57) = 5.98\ \mathrm{eV}. \tag{14}$$

If we allow for a structural relaxation in the larger cluster we get

$$\Delta E_{fin\text{-}size}^{F\ struct\text{-}relax} = 76E_{CaF_2} + E_{Ca_{32}F_{63}} - E_{Ca_{108}F_{215}}^{struct\text{-}relax}$$
$$= -1902.59 - (-1910.42) = 7.83\ \mathrm{eV}, \tag{15}$$

where E_{CaF_2} is the total energy of a single CaF_2 unit cell and $E_{Ca_{32}F_{63}}$ is the total energy of the cluster from Sec. V A and $E_{Ca_{108}F_{215}}$ is the total energy of the large superstructure. The differences in energy result from an interaction between a single charge center and its neighbors due to the periodic boundary conditions of the underlying system. The major part (5.98 eV) stems from the electronic interaction whereas only a small part (7.83 eV−5.98 eV=1.85 eV) stems from an interaction between the different lattice distortions around each individual charge center. Therefore the major contribution of the relatively large energy difference originates from the long-range Coulomb interaction between the charge center and its neighbors due to the periodic boundary conditions.

For the *H* center we obtain from a similar calculation for the electronic part only

$$\Delta E_{fin\text{-}size}^{H\ elec\text{-}relax} = 76E_{CaF_2} + E_{Ca_{32}F_{65}} - E_{Ca_{108}F_{217}}^{elec\text{-}relax}$$
$$= -1911.67 - (-1912.82) = 1.15\ \mathrm{eV}, \tag{16}$$

and for the structural relaxation we get

$$\Delta E_{fin\text{-}size}^{H\ struct\text{-}relax} = 76E_{CaF_2} + E_{Ca_{32}F_{65}} - E_{Ca_{108}F_{217}}^{struct\text{-}relax}$$
$$= -1911.67 - (-1913.13) = 1.39\ \mathrm{eV}. \tag{17}$$

In this case as well the electronic part (1.15 eV) as well as the structural part is due to the interaction between lattice distortions (1.42 eV−1.15 eV=0.27 eV).

The reason why finite-size effects are much smaller for the *H* center is due to the more efficient screening of the Coulomb charges in the case of the *H* center. In this case there is a much larger but also much stronger localized lattice distortion which leads to more strongly localized electronic

wave functions of the defect level. This can be also seen by the weak but still present dispersion of the defect level in Figs. 2 and 4.

VI. CONCLUSION

In the present paper we calculate the ground state of the trapped electron (bare F center) and of the trapped hole (bare H center) in CaF_2. These charge centers are the elementary excitations which are needed to understand the interaction between CaF_2 and DUV radiation. Since DUV radiation can even in an ideal crystal excite electron-hole pairs via a two-photon process, the electron or the hole can localize, gaining energy via a lattice distortion. The formation energy for a F-H pair is, however, unevenly shared between the electron and the hole. This is the reason why already in an as-grown crystal a finite number of F centers of the order of 5 ppm is present, while there are no H centers present. This explains why in fluorite crystals there are F centers observed but H centers are observed only if they are stabilized by impurities. Calculating the lattice distortion around the F center, we found no surprise. However, when investigating the lattice distortion around the H center we found that the state of smallest total energy is a configuration where the direction connecting the two interstitial F ions points along the 110 direction of the crystal. Further, the charge is distributed rather around in an F_4^{3-} complex rather than in an F_2^- complex. For the important problem of radiation stability of CaF_2 under intense excimer laser radiation, the trapping of these charge centers on impurity ions has to be considered. The radiation stability of CaF_2 is of extreme importance for the optical microlithography for structuring semiconductors.

ACKNOWLEDGMENTS

M.L. thanks J. M. Spaeth and A. Engel for fruitful and stimulating discussions.

APPENDIX A: TEST OF NUMERICAL ACCURACY DUE TO PLANE-WAVE CUTOFF

In a strongly ionic crystal like CaF_2 there is a large spatial fluctuation of the electron charge. Therefore it is expected that a large number of plane waves (in k space) has to be used to achieve a numerical accuracy which allows quantitative predictions.

In Fig. 8 we have plotted the total energy of a CaF_2 system as a function of the plane-wave cutoff. In Fig. 9 we show the resulting lattice constants after a structural relaxation. For cutoff energies of 500 eV and larger the system starts to saturate. To minimize calculation time we have used a plane-wave cutoff of 500 eV throughout the calculations of the larger clusters for the calculation of charge centers and impurities in CaF_2. In Fig. 9 the resulting lattice constant of CaF_2 is shown as a function of the cutoff energy.

APPENDIX B: SPLITTING OF ENERGY LEVELS OF CHARGE CENTER DUE TO SYMMETRY CONSIDERATIONS

In this appendix we give a few thoughts about symmetry, which are based on group theoretical arguments. We assume

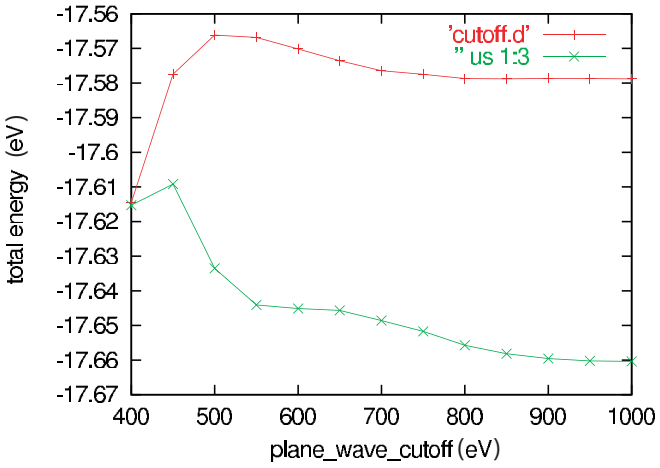

FIG. 8. (Color online) The total energy for CaF_2 as a function of plane-wave cutoff. For cutoff energies of 500 eV the system starts to saturate. The upper (red) curve shows the result without structural relaxation and the lower (green) curve shows the result with structural relaxation of the elementary cell.

that a charge center forms a kind of hydrogen atom which is perturbed by the symmetry of the underlying crystalline lattice. In the case of the F center this is obvious since the fluor vacancy forms a net positive charge in which the excess electron is localized due to Coulomb attraction. The point symmetry group of the F center is tetrahedron symmetry T_d. In the case of the H center this is less obvious. The excess fluorine ion brings a negative charge which is compensated by a positive charge which is localized among the four F ions as shown in Fig. 6. The point symmetry of the whole H center is C_{2v}.

The optically allowed transitions within the hydrogen atom are given by well-known rules which follow from symmetry considerations in the rotation group, $O(3)=R+C_i$. The angular part of the eigenfunctions in the $O(3)$ group are the spherical harmonics, D_l^p, where l is the angular index of the spherical harmonics and p the parity (+ or −) of the wave function. Under the perturbation of the external field these

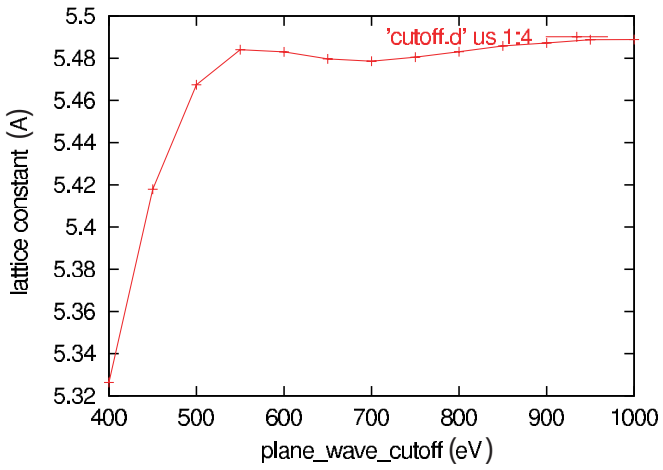

FIG. 9. (Color online) The lattice constant of CaF_2 after structural relaxation is plotted as a function of plane-wave cutoff.

TABLE III. For the first four excitations of a charge center we give the relevant part of the correlation table for a splitting of the energy levels with respect to the symmetry of the F and the H centers.

$O(3)=R\times C_i$	F center T_d	H center C_{2v}
$D_0^{\pm}$	$A_{1/2}$	$A_{1/2}$
$D_1^{\pm}$	$T_{1/2}$	$A_{2/1}+B_1+B_2$
$D_2^{\pm}$	$E+T_{2/1}$	$A_{1/2}+2B_1+2B_2$
$D_3^{\pm}$	$A_{2/1}+T_1+T_2$	$A_{1/2}+2A_{2/1}+2B_1+2B_2$
$D_4^{\pm}$	$A_{1/2}+E+T_1+T_2$	$3A_{1/2}+2A_{2/1}+2B_1+2B_2$

$(2l+1)$ times degenerate eigenvalues split in a well defined way. This is given in correlation tables which can be found in standard textbooks of group theory.[26] In Table III we give the part of the correlation table which is relevant for the symmetry of the charge centers. From Table III we learn the following important things: (i) the splitting of the energy levels in the excited states, and second, the numbers of independent parameters which are required to expand the crystal field up to fourth order in l. In the case of the F center only the second excited state splits into a twofold (E) and a threefold $(T_{2/1})$ degenerate energy level. The third excited state splits into three levels, one highly symmetric $A_{2/1}$ and two levels which are each threefold degenerate T_1 and T_2. In the case of the H center all degeneracies up to fourth order are canceled, already the first excited state splits into three nondegenerate energy levels $A_{2/1}$, B_1, and B_2. The second excited energy level splits into five different levels and so on. By (ii) counting the number of A_1 representations we know the number of independent parameters which are needed for an expansion of the crystal field up to fourth order in l. For the F center these are only three parameters whereas for the H-center with its much lower symmetry 11 parameters are required.

[1] J. H. Burnett, Z. H. Levine, and E. L. Shirley, Phys. Rev. B **64**, 241102(R) (2001).
[2] M. Letz, L. Parthier, A. Gottwald, and M. Richter, Phys. Rev. B **67**, 233101 (2003).
[3] E. W. Hayes, *Crystals with the Fluorite Structure* (Clarendon Press, Oxford, 1974), p. 102.
[4] *Physics of Color Centers*, edited by W. B. Fowler (Academic Press, New York, 1968).
[5] T. Tsujibayashi, M. Watanabe, O. Arimoto, M. Itoh, S. Nakanishi, H. Itoh, S. Asaka, and M. Kamada, J. Lumin. **87-89**, 254 (2000).
[6] Ch. Görling, U. Leinhos, and K. Mann, Opt. Commun. **249**, 319 (2005).
[7] T. Tomiki and T. Miyata, J. Phys. Soc. Jpn. **27**, 658 (1969).
[8] J. Barth, R. L. Johnson, M. Cardona, D. Fuchs, and A. M. Bradshaw, Phys. Rev. B **41**, 3291 (1990).
[9] R. T. Williams, M. N. Kabler, W. Hayes, and J. P. Stott, Phys. Rev. B **14**, 725 (1976).
[10] R. Lindner, R. T. Williams, and M. Reichling, Phys. Rev. B **63**, 075110 (2001).
[11] M. Mizuguchi, H. Hosono, and H. Kawazoe, J. Opt. Soc. Am. B **16**, 1153 (1999).
[12] K. Tanimura, Phys. Rev. B **63**, 184303 (2001).
[13] Ch. Mühlig, W. Triebel, G. Töpfer, and A. Jordanov, Proc. SPIE **4932**, 458 (2003).
[14] L. P. Cramer, T. D. Cumby, J. A. Leraas, S. C. Langford, and J. T. Dickinson, J. Appl. Phys. **97**, 103533 (2005).
[15] E. W. Hayes, *Crystals with the Fluorite Structure* (Ref. 3), p. 240.
[16] V. N. Kuzovkov, E. A. Kotomin, and W. von Niessen, Phys. Rev. B **58**, 8454 (1998).
[17] K. Atobe, J. Chem. Phys. **71**, 2588 (1979).
[18] G. Kresse and J. Furthmüller, Phys. Rev. B **54**, 11169 (1996).
[19] M. Kim, Y. Zhao, A. J. Freeman, and W. Mannstadt, Appl. Phys. Lett. **84**, 3579 (2004).
[20] K. Schmalzl, D. Strauch, and H. Schober, Phys. Rev. B **68**, 144301 (2003).
[21] R. Khenata, B. Daoudi, M. Salnoun, H. Batlache, M. Rerat, A. H. Reshak, B. Bouhafs, H. Abid, and M. Driz, Eur. Phys. J. B **47**, 63 (2005).
[22] J. M. Spaeth and S. Schweizer, internal report, SCHOTT AG, Mainz, Germany, 2004.
[23] H. Pick, in *Optical Properties of Solids*, edited by F. Abeles (North-Holland, Amsterdam, 1972), p. 653.
[24] H. Shi, R. I. Eglitis, and G. Borstel, Phys. Rev. B **72**, 045109 (2005).
[25] A. V. Puchina, V. E. Puchin, E. A. Kotomin, and M. Reichling, Solid State Commun. **106**, 285 (1998).
[26] M. Hamermesh, *Group Theory and its Application to Physical Systems* (Dover, New York, 1990).